Neuron, Vol. 20, 895–904, May, 1998, Copyright ©1998 by Cell Press

A Synaptic Ras-GTPase Activating Protein (p135 SynGAP) Inhibited by CaM Kinase II

Hong-Jung Chen, Michelle Rojas-Soto, Asako Oguni, and Mary B. Kennedy*
Division of Biology
California Institute of Technology
Pasadena, California 91125

Summary

Ca^{2+} influx through N-methyl-D-aspartate– (NMDA–) type glutamate receptors plays a critical role in synaptic plasticity in the brain. One of the proteins activated by the increase in Ca^{2+} is CaM kinase II (CaMKII). Here, we report a novel synaptic Ras-GTPase activating protein (p135 SynGAP) that is a major component of the postsynaptic density, a complex of proteins associated with synaptic NMDA receptors. p135 SynGAP is almost exclusively localized at synapses in hippocampal neurons where it binds to and closely colocalizes with the scaffold protein PSD-95 and colocalizes with NMDA receptors. The Ras-GTPase activating activity of p135 SynGAP is inhibited by phosphorylation by CaMKII located in the PSD protein complex. Inhibition of p135 SynGAP by CaMKII will stop inactivation of GTP-bound Ras and thus could result in activation of the mitogen-activated protein (MAP) kinase pathway in hippocampal neurons upon activation of NMDA receptors.

Introduction

Ca^{2+}/calmodulin-dependent protein kinase II (CaMKII) is expressed at high levels in hippocampus and cortex (Erondu and Kennedy, 1985) and is important for induction of long-term potentiation, a long-lasting enhancement of excitatory transmission believed to participate in the encoding of memory (Silva et al., 1992; Mayford et al., 1995). CaMKII is activated in hippocampal neurons by the rise in intracellular Ca^{2+} that follows stimulation of NMDA receptors (Fukunaga et al., 1992, 1993; Ouyang et al., 1997). It is concentrated in a complex of proteins known as the postsynaptic density (PSD) (Kennedy et al., 1983; Kelly et al., 1984), which contains a set of signal-transduction molecules that copurify in a tight complex and colocalize with NMDA receptors at synapses (Apperson et al., 1996; Kennedy, 1997; Rao and Craig, 1997). Many of these proteins appear to be tethered to the NMDA receptor via the scaffold protein PSD-95 (Kornau et al., 1995; Sheng, 1996; Niethammer et al., 1996; Irie et al., 1997).

Activation of NMDA receptors in hippocampal neurons also activates mitogen-activated protein (MAP) kinase and this activation is important for induction of long-term potentiation (Bading and Greenberg, 1991; English and Sweatt, 1996, 1997). It can lead ultimately to stimulation of transcription in the nucleus (Bading et al., 1993; Ghosh and Greenberg, 1995; Xia et al., 1996). However, the molecular mechanism(s) that couple the rise in Ca^{2+} at the synapse to MAP kinase activation are not yet clear (Farnsworth et al., 1995; Finkbeiner and Greenberg, 1996). The best understood means of activating the MAP kinase cascade in most cells involves generation of the GTP-bound form of Ras, which recruits Raf kinase to the membrane where it initiates a protein phosphorylation cascade leading to activation of MAP kinase (Cobb and Goldsmith, 1995). Activation of Ras is usually coupled to receptors through adapter proteins, such as Shc and Grb2, that bind to phosphorylated tyrosines and couple Ras guanine nucleotide exchange factors (GEFs) with Ras. GEFs catalyze exchange of GTP for GDP bound to Ras. Equally important for Ras regulation are the GTPase activating proteins (GAPs) (Trahey et al., 1988; Vogel et al., 1988; Wigler, 1990; Downward et al., 1990). Ras has slow intrinsic GTPase activity that hydrolyzes bound GTP to form GDP. GAP proteins enhance the rate of GTP hydrolysis and catalyze rapid inactivation of Ras. Only two major classes of mammalian RasGAPs have been described previously, p120 RasGAP and Neurofibromin-1 (NF-1) (Wigler, 1990; Downward et al., 1990).

To determine the targets of CaMKII at the postsynaptic site, we have used microchemical sequencing and cDNA cloning to identify additional prominent proteins in the PSD complex that are phosphorylated by CaMKII. One major novel protein identified in this manner, p135 SynGAP, which is described here, represents a third class of mammalian RasGAPs. It is expressed primarily in brain and is localized to synapses containing NMDA receptors. It constitutes ~1%–2% of total protein in isolated PSDs and is rapidly phosphorylated upon activation of CaMKII in the PSD. Its carboxyl terminus contains a tS/TXV motif that can bind to the PDZ domains in PSD-95, and it coprecipitates with PSD-95 from isolated PSDs. Phosphorylation of p135 SynGAP by CaMKII reversibly inhibits GAP activity and may represent an important link between activation of NMDA receptors and activation of the MAP kinase pathway.

Results

PCR Cloning Based on Tryptic Peptide Sequences

Four individual protein bands were electroeluted and concentrated from SDS-gels of isolated PSDs from rat forebrain (Figure 1). Tryptic peptides were obtained from each of the bands and individual peptides were purified by high pressure liquid chromatography HPLC and sequenced by a combination of mass spectrometry and gas phase Edman degradation. Sequences of peptides from the highest molecular weight band (160 kDa) identified the major protein as neurofilament-M. A total of 18 distinct peptide sequences (Figure 1) were obtained from the three lower molecular weight bands (~150 kDa, ~140 kDa, and ~130 kDa). Combinations of sense and antisense oligonucleotides were designed based upon the peptide sequences and used in a pairwise fashion to amplify sequences from rat forebrain mRNA by reverse-transcription polymerase chain reaction (RT-PCR) (Figure 2; Apperson et al., 1996). Several cDNAs hybridizing

*To whom correspondence should be addressed.

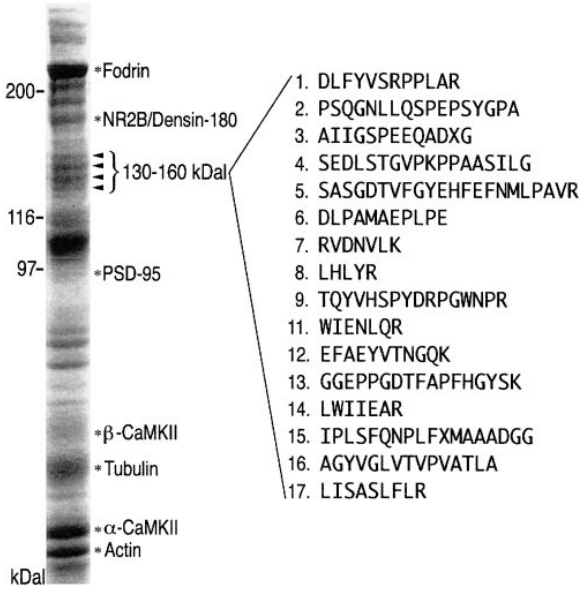

Figure 1. Tryptic Sequences of p135 SynGAP Obtained from Isolated PSDs

Isolated PSDs (One-Triton, 60 μg) were fractionated by SDS-PAGE and proteins were stained with Coomassie blue. Asterisks indicate the positions of previously identified proteins (Kennedy, 1997). Arrowheads indicate protein bands that were excised and electroeluted from preparative gels as described in Experimental Procedures. Peptide sequences listed on the right were obtained as described in Experimental Procedures. Four sequences were obtained from more than one of the three lower protein bands, indicating that the major proteins present in these bands are closely related to each other. Positions of molecular weight markers are shown on the left.

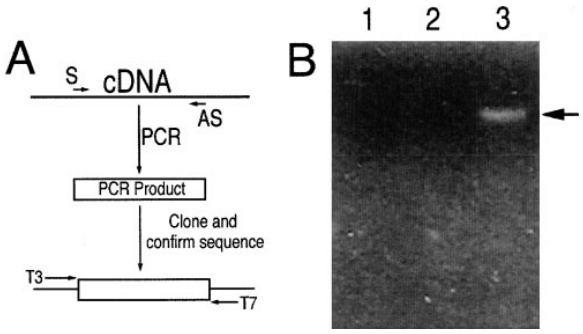

Figure 2. PCR Cloning of p135 SynGAP

(A) Sense ("S") and antisense ("AS") degenerate oligonucleotides were designed based upon peptide sequences obtained from electroeluted proteins (Figure 1). Combinations of sense and antisense oligonucleotides were used as PCR primers to amplify rat forebrain first-strand cDNAs as described in Experimental Procedures. PCR products were sequenced to confirm the fidelity of the amplified sequences.

(B) DNA from PCR reactions was fractionated on a 1.2% agarose gel and stained with ethidium bromide. PCR products are shown from reactions with (lane 1) only the S primer encoding peptide 9, (lane 2) only the AS primer encoding peptide 14, (lane 3) a combination of the S primer encoding peptide 9 and AS primer encoding peptide 14. PCR product (arrow) is 723 bp.

with a 723 bp PCR product were selected from a cDNA library, sequenced, and assembled into the complete coding sequence as described in Experimental Procedures.

Sequence and Domain Structure of p135 SynGAP

The deduced amino acid sequence (Figure 3A) contains 16 of the 18 original peptides, indicating that the encoded protein is the principal protein present in the bands visible on the SDS gel (Figure 1). Two apparent splice variants were found among the cDNA clones, one at the amino terminus and one at the carboxyl terminus. The combinations would encode four variants of molecular weights, 134, 137, 140, and 143. The mass of a seventeenth peptide (Figure 1, number 3) determined by mass spectrometry (2034 Da) matches that of a predicted tryptic peptide sequence that includes a portion of the carboxy-terminal splice variant (Figure 3A, variant b).

The sequence contains four regions homologous to previously identified protein motifs (Figure 3B). Most notable is the RasGAP motif from positions 393 to 717 (Figure 3C). Its sequence is 30% identical to p120 RasGAP and it contains the FLR... PA... P motif diagnostic for RasGAPs (Scheffzek et al., 1996). The amino-terminal segment contains a putative PH domain, which may attach the protein to the membrane (Lemmon et al., 1997), and a region 31% identical to the C2 domain of p120 GAP, a motif that mediates binding to phospholipid and/or Ca^{2+} in synaptotagmin and protein kinase C (Südhof and Rizo, 1996). Two of the putative splice variants end in QTRV, conforming to the consensus sequence tS/TXV that can bind to the second and third PDZ domains of the scaffold protein PSD-95 (Kornau et al., 1995; Sheng, 1996; Niethammer et al., 1996; Irie et al., 1997). A proline-rich region between positions 770 and 800 may form a binding site for SH3 domains (Cohen et al., 1995).

p135 SynGAP Is Most Highly Expressed in Brain, Forms a Complex with PSD-95, and Localizes to Glutamatergic Synapses

The message encoding p135 SynGAP is expressed at higher levels in brain than in other tissues (Figure 4). Furthermore, within neurons the protein is highly localized to synapses. Western blots of subcellular fractions from rat forebrain made with antibodies against p135 SynGAP reveal that it is enriched in isolated PSDs even after extraction with the relatively harsh detergent N-lauroyl sarcosinate (Figure 5A). Carboxyl termini of SynGAP containing either the terminal sequence QTRV (+QTRV) or the alternatively spliced terminal sequence PRHG (−QTRV; Figure 3A) were expressed in the yeast bait vector, pAS2-1, and their ability to interact with intact PSD-95 was tested in a yeast two-hybrid assay (Figure 5C). As predicted, the recombinant carboxy-terminal tail containing the sequence QTRV interacts strongly with PSD-95 in the assay, whereas the recombinant carboxyl terminus containing the predicted alternatively spliced sequence missing QTRV does not interact with PSD-95 in this assay. Immunoprecipitation of p135 SynGAP from isolated PSDs results in specific coprecipitation of PSD-95 (Figure 5B), supporting the notion that p135 SynGAP is present in brain in a complex with PSD-95 as predicted by the yeast two-hybrid results and the presence of the

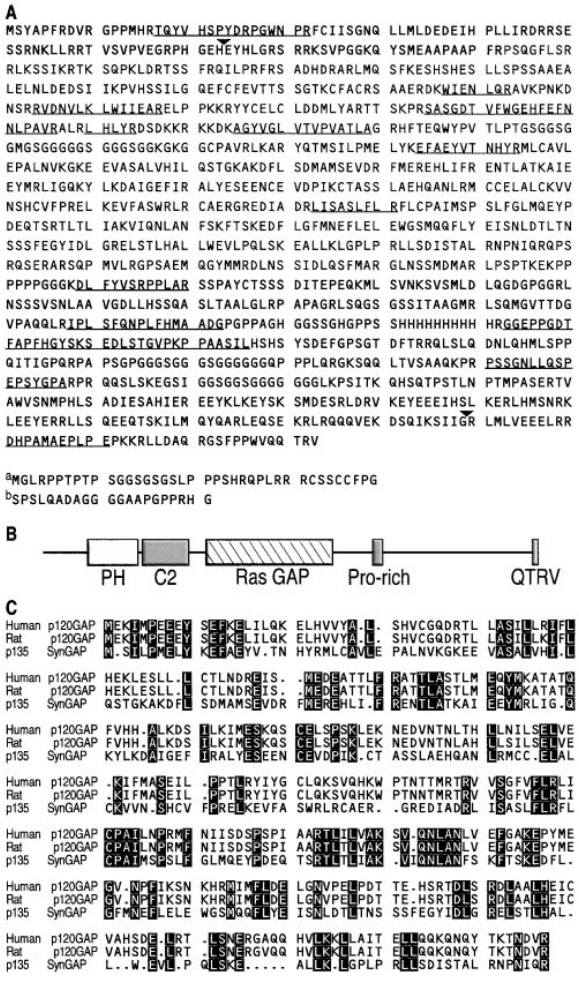

Figure 3. p135 SynGAP Sequence

(A) Deduced protein sequence of p135 SynGAP. A 723 bp PCR product that encoded two complete peptides at its ends and a third peptide (number 11) in between was obtained with primers encoding peptides 9 and 14 (Figure 1). It was purified, radiolabeled, and used to screen a rat brain cDNA library. Twelve positive clones were sequenced and assembled into a complete open reading frame containing a Kozak consensus sequence three bases upstream of the methionine start codon (GenBank Accession number AF048976). Sequences corresponding to tryptic peptides (Figure 1) are underlined. For peptides 2–6, 12, and 15, a few amino acid calls did not match; however, the masses determined by mass spectrometry matched the predicted tryptic peptides exactly. Arrowheads indicate putative splice junctions; a and b designate amino-terminal and carboxy-terminal splice variants, respectively (GenBank Accession numbers AF053938 and AF055883).

(B) Domain structure of p135 SynGAP. Abbreviations are: PH, pleckstrin homology domain (125–232); C2, C2 domain (239–330); RasGAP, RasGAP domain, (393–717); Pro-rich, proline-rich domain (770–800); QTRV, tS/TXV motif.

(C) Comparison of RasGAP domains. The RasGAP domains of human p120 RasGAP, rat p120 RasGAP, and p135 SynGAP were aligned with the Pile-Up program (GCG). Residues identical in all three sequences are highlighted in black. Dots indicate gaps in the alignment.

tS/TXV motif (see also Kim et al., 1998). An antibody raised against the longer of the alternative amino-terminal sequences (Figure 3A) precipitates only the two

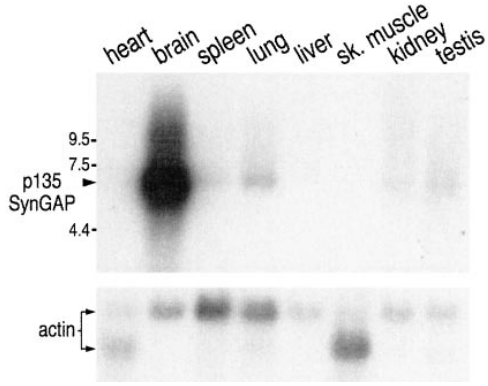

Figure 4. Expression of p135 SynGAP in Tissues

A Multiple Tissue Northern blot (Clontech) was probed with ^{32}P-labeled probe for p135 SynGAP (bases 251–767) according to the manufacturer's protocol and then stripped and probed with ^{32}P-labeled human β-actin cDNA supplied by Clontech. The blot with p135 SynGAP was exposed for 18 hr and with actin for 2 hr for detection by autoradiography. Positions of RNA size markers are indicated on the left.

largest of the four protein bands recognized by an antibody against the GAP domain (Figure 5B), suggesting that both potential amino-terminal variants are present in isolated PSDs. The NR2B subunit of the NMDA receptor has been shown to form a complex with PSD-95 and to coimmunoprecipitate with it under some conditions (Kornau et al., 1995; Lau et al., 1996). Only a small amount of NR2B coimmunoprecipitated with p135 SynGAP under our conditions, suggesting that the complex between p135 SynGAP and PSD-95 may be more stable than that between NR2B and PSD-95. This perhaps reflects the fact that the tail of p135 SynGAP can interact with all three PDZ domains of PSD-95 (Kim et al., 1998). NR2B and p135 SynGAP would likely be held within a large complex in the PSD because of the multimerization of PSD-95 to form a three-dimensional network (Hsueh et al., 1997). p135 SynGAP is highly localized to synapses as revealed by immunocytochemical staining with anti-p135 SynGAP antibodies (Figure 6A). It colocalizes with NR2B (Figures 6B and 6C) and with PSD-95 (Figures 6D and 6E), providing support for the hypothesis that it is present in a complex with the NMDA receptor.

p135 SynGAP Is a Prominent Substrate for CaMKII in Isolated PSDs

Proteins of molecular weights similar to the SynGAP are phosphorylated by CaMKII in isolated PSDs (Figure 7A). The phosphorylation is ~90% blocked in the presence of inhibiting antibodies against CaMKII. Approximately 70% of the ^{32}P-labeled protein in this molecular weight range is specifically immunoprecipitated by an anti-p135 SynGAP antibody, indicating that it is a major substrate for CaMKII in the PSD (Figure 7B). The sequence of p135 SynGAP contains 29 consensus sites (RXXS/T) for phosphorylation by CaMKII. The SynGAP protein bands can be visualized in SDS gels of the PSD fraction by staining with Coomassie blue (Figure 1) and also in gels of immunoprecipitates. Therefore, we can estimate the quantity of SynGAP protein precipitated from the

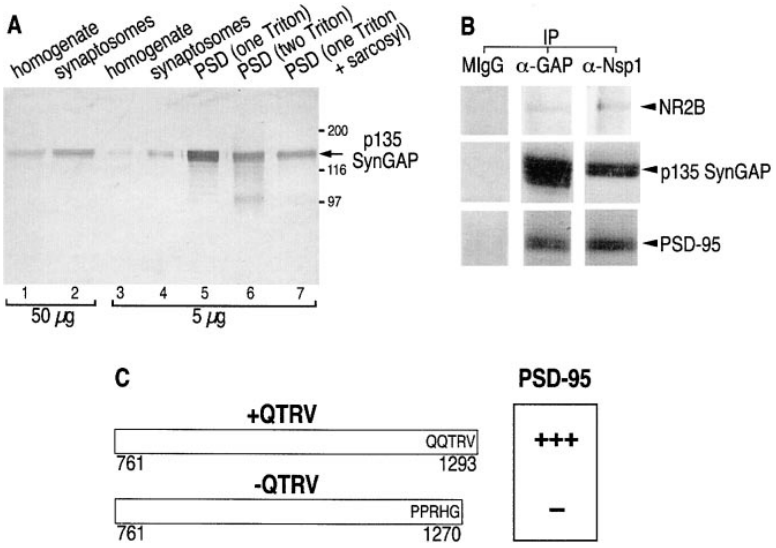

Figure 5. Association of p135 SynGAP with PSD-95 in Isolated PSDs

(A) p135 SynGAP is enriched in the PSD fraction. Rat forebrain homogenate and synaptosomes (50 μg and 5 μg) and isolated PSDs (5 μg each) extracted once with Triton (one Triton), twice with Triton (two Triton), or once with Triton followed by N-lauroyl sarcosinate (one Triton + sarcosyl) were fractionated by SDS-PAGE. Enrichment of p135 SynGAP in isolated PSDs is revealed by immunoblotting with anti-GAP antibody.

(B) Coimmunoprecipitation of PSD-95 with p135 SynGAP. Mouse antibodies against the GAP domain of SynGAP, against residues 17–85 located in an alternatively spliced region, and nonimmune Mouse IgG were used to immunoprecipitate p135 SynGAP from isolated PSDs as described in Experimental Procedures. Western blots of the immunoprecipitates were made with antisera against proteins listed on the right. Densin-180, another PSD protein, was not detected in the immunoprecipitates by Western blotting (data not shown).

(C) SynGAP containing the tS/TXV motif associates with PSD-95 in the yeast two-hybrid assay. Two yeast two-hybrid bait constructs were tested for interaction with full-length PSD-95 as described in Experimental Procedures. The +QTRV construct interacts strongly, whereas the −QTRV construct does not.

PSD fraction by comparison with the intensity of staining of known protein standards. Using these estimates, we calculate that incubation of isolated PSDs for 2 min under phosphorylating conditions results in the incorporation of ~4 moles of phosphate/mol SynGAP.

The Ras-GTPase Activating Activity of p135 SynGAP Is Inhibited by Phosphorylation by CaMKII

We tested whether RasGAP activity can be measured in isolated PSDs and whether phosphorylation by CaMKII alters the activity. Addition of 30 μg of isolated PSDs containing ~2 pmol p135 SynGAP stimulates hydrolysis of GTP bound to Ras 5-fold in a 10 min assay and 3-fold in a 30 min assay (Figure 8A). The activity corresponds to an estimated turnover number for SynGAP-bound Ras of ~10/s, a rate that compares favorably with that of p120 RasGAP. We detected the p120 RasGAP protein in Western blots of synaptosomes but found that it is absent from isolated PSDs (data not shown). The GAP activity in isolated PSDs is inhibited 75%–78% by addition of a mouse antibody against the GAP domain of p135 SynGAP (Figure 8A) and is unaffected by addition of nonimmune mouse IgG, indicating that p135 SynGAP is indeed responsible for the GAP activity.

When isolated PSDs are prephosphorylated for 2 min by activation of endogenous CaMKII, GAP activity is inhibited 80%–93% in a 10 min assay and 63%–85% in a 30 min assay (Figure 8A). The inhibition of GAP activity is blocked if the prephosphorylation is carried out in the presence of inhibiting antibodies against CaMKII, indicating that phosphorylation by CaMKII is necessary for the inhibition. Because the SynGAP molecule is a good substrate for CaMKII in isolated PSDs (Figure 7), the most straightforward interpretation of these results is that phosphorylation of SynGAP itself inhibits GAP activity. However, it is also possible that phosphorylation by CaMKII of an unknown SynGAP-interacting protein in the isolated PSDs causes the inhibition.

Proteins phosphorylated by CaMKII in PSDs are fully dephosphorylated 2 min after the kinase reaction is stopped by addition of EGTA to chelate free calcium (Figure 7A), presumably because of the presence of protein phosphatase 1 in the isolated PSDs (Shields et al., 1985). This dephosphorylation is inhibited by addition of sodium pyrophosphate ($NaPP_i$; Figure 7A), so we added $NaPP_i$ to the GAP assays shown in Figure 8A. To test whether inhibition of GAP activity by CaMKII phosphorylation is reversible, we compared GAP activity of phosphorylated PSDs in the presence and absence of $NaPP_i$ (Figure 8B). When phosphorylated PSDs are added to the GAP assay in the absence of $NaPP_i$, GAP activity returns rapidly to the level of unphosphorylated PSDs, demonstrating that the inhibition by phosphorylation is fully reversible. $NaPP_i$ has no effect on GAP activity of unphosphorylated PSDs.

Discussion

Our data reveal a novel mammalian RasGAP that is expressed principally in brain and is highly localized to glutamatergic synapses, apparently by association with the postsynaptic scaffold protein PSD-95. We have shown that p135 SynGAP is reversibly inhibited by the action of CaMKII within isolated PSDs, either through direct phosphorylation of SynGAP itself, which is readily phosphorylated by CaMKII, or through phosphorylation of an unidentified third protein in the isolated PSDs that influences the GAP activity. CaMKII is activated in hippocampal neurons by Ca^{2+} influx through NMDA receptors (Fukunaga et al., 1992, 1993; Ouyang et al., 1997). Therefore, a reasonable hypothesis is that within the PSD complex one of the consequences of this activation is inhibition of p135 SynGAP.

Activation of MAP kinase by the NMDA receptor is necessary for some forms of synaptic plasticity (Bading and Greenberg, 1991; English and Sweatt, 1996, 1997),

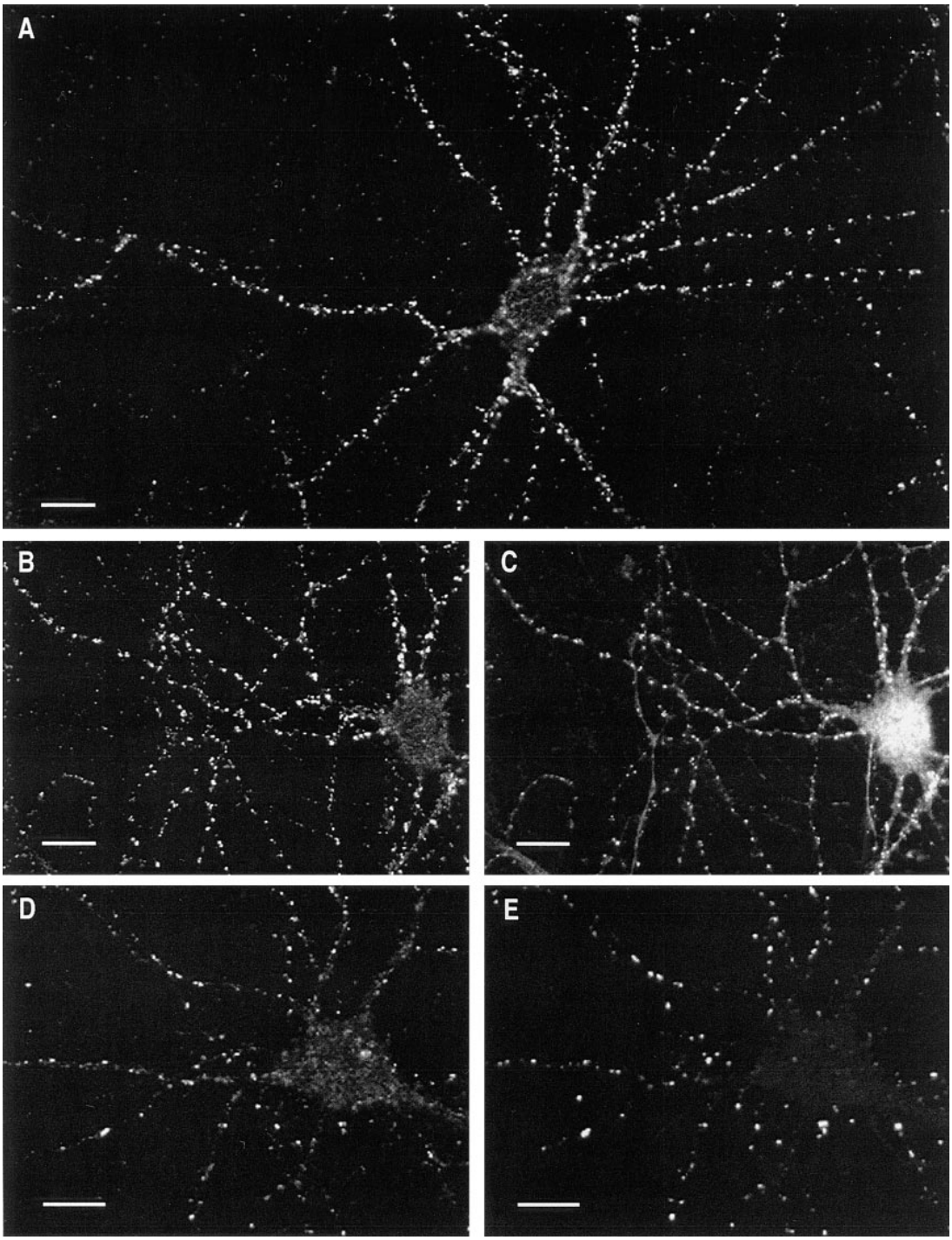

Figure 6. Immunocytochemical Localization of p135 SynGAP at Glutamatergic Synapses in Dissociated Hippocampal Neurons

(A) Hippocampal neuron stained with anti-GAP antibody. Hippocampal neurons were dissociated at embryonic day 18, cultured for 2 weeks, and stained with antiserum as described in Experimental Procedures. Labeling of neurons is eliminated by preabsorption of the antiserum with its antigen (data not shown).

(B and C) Neuron double stained with anti-GAP (B) and anti-NR2B (C).

(D and E) Neuron double stained with anti-GAP (D) and anti-PSD-95 (E).

Scale bars, 10 μm.

but the mechanism by which Ca^{2+} influx through the NMDA receptor activates MAP kinase has been mysterious (Bading et al., 1993; Ghosh and Greenberg, 1995; Farnsworth et al., 1995; Finkbeiner and Greenberg, 1996; Xia et al., 1996). Much emphasis has been placed upon the study of mechanisms that activate the MAP kinase

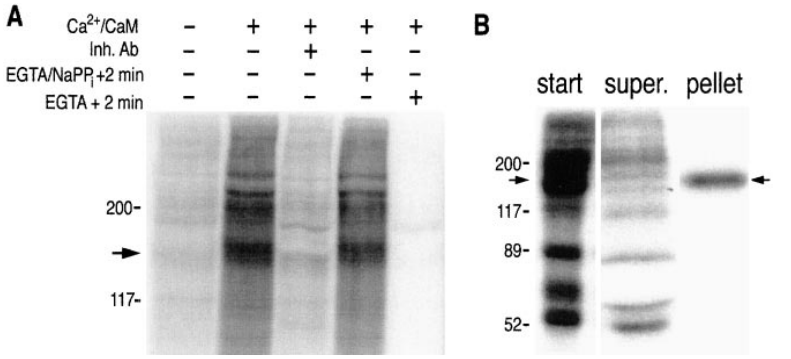

Figure 7. Phosphorylation of p135 SynGAP by CaMKII in Isolated PSDs

(A) Phosphorylation of isolated PSDs by endogenous CaMKII. PSDs (One-Triton, 40 μg) were phosphorylated in the presence or absence of Ca^{2+}, calmodulin, and specific inhibiting monoclonal antibodies against CaMKII (Ab 4A11 and 6E9) for 2 min as described in Experimental Procedures. Reactions in the first three lanes were stopped by addition of SDS sample buffer. Reactions in the right two lanes were stopped by addition of a final concentration of 2 mM EGTA to chelate Ca^{2+} and 20 mM $NaPP_i$ to inhibit phosphatases, or 2 mM EGTA alone, and then incubated for an additional 2 min before addition of SDS sample buffer. Positions of molecular weight markers are shown on the left.

(B) Immunoprecipitation of phosphorylated p135 SynGAP from isolated PSDs. PSDs (40 μg) were phosphorylated as in (A). p135 SynGAP was immunoprecipitated with anti-GAP antibody. Amounts of each fraction equivalent to 5 μg of phosphorylated PSDs were fractionated by SDS-PAGE. Abbreviations: start, precleared phosphorylated PSDs; super., supernatant from the immunoprecipitation; pellet, immunoprecipitated pellet. Arrows indicate positions of p135 SynGAP.

cascade through formation of active Ras-GTP; however, an interesting example of activation of the MAP kinase cascade by inhibition of p120 RasGAP occurs in the immune system. Upon T-cell activation by antigen, Ras is activated by a decrease in the activity of p120 RasGAP thought to be mediated by protein kinase C (Wigler, 1990; Downward et al., 1990). Our data suggest that, in similar fashion, inactivation of p135 SynGAP by CaMKII in the PSD complex at glutamatergic synapses can release a brake on the tonic activation of Ras by synaptic tyrosine kinases (Figure 9). Many tyrosine kinases have been shown to influence synaptic events in vivo (Grant et al., 1992; Kang and Schuman, 1995; Lu et al., 1998), although the precise localization of these kinases has not been established. Several growth-factor receptor tyrosine kinases occur in the hippocampus and throughout the central nervous system, including those for BDNF, NT3, and NGF, which have been implicated in various forms of synaptic plasticity during development and in the adult brain (Prakash et al., 1996; Schuman, 1997; Cabelli et al., 1997; McAllister et al., 1997). Src family kinases have also been implicated in synaptic plasticity in the hippocampus (Grant et al., 1992; Lu et al., 1998) and can activate Ras through interaction with the coupling proteins Shc and Grb2 (Rozakis-Adcock et al., 1992; Nakamura et al., 1998). The ability of a phosphatase associated with isolated PSDs to reverse rapidly phosphorylation of p135 SynGAP and other PSD proteins (Figures 7A and 8B), suggests that steady state levels of SynGAP activity may fluctuate rapidly, providing tight regulation of Ras-GTP.

p135 SynGAP is a relatively abundant protein within the postsynaptic complex of signal transduction molecules associated with the NMDA receptor and held together in part by interaction with the scaffold protein PSD-95. It is also a prominent substrate for CaMKII in isolated PSDs. Therefore, inhibition of its GAP activity is likely to be an important consequence of activation of CaMKII by the NMDA receptor. The presence of p135 SynGAP at glutamatergic synapses may help to explain the activation of the MAP kinase cascade that accompanies NMDA receptor activation in the hippocampus (Bading and Greenberg, 1991; English and Sweatt, 1996, 1997) and, furthermore, may add a new form of coincidence detection to the repertoire of the NMDA receptor.

Experimental Procedures

Purification of Tryptic Peptides from the Postsynaptic Density

The One-Triton PSD fraction was prepared as described previously (Carlin et al., 1980; Cho et al., 1992). PSDs (40 mg) were fractionated on 30 preparative 7.5% SDS-polyacrylamide gels. Proteins from each of the four visible bands indicated by arrowheads in Figure 1 were electroeluted into ~3 ml as described previously (Moon et al., 1994) and then further concentrated in a Speed-Vac concentrator to ~300 μl containing ~200 μg protein. Sixty micrograms of each of the four concentrated pools were repurified on two 7.5% SDS gels. The two gel strips were chopped into 3 mm squares. Proteins were trypsinized in the gel pieces as described (Hellman et al., 1995). Peptides were fractionated by HPLC on a C18 reverse-phase column (Omkumar et al., 1996). Peak fractions were collected manually and analyzed by matrix-assisted, laser desorption ionization, time-of-flight (MALDI-TOF) mass spectrometry. Pure peptides were sequenced by automated gas phase Edman degradation. Mass spectrometry and peptide sequencing were performed by the Protein/Peptide Micro-Analytical Laboratory at Caltech.

Selection of cDNAS Encoding p135 SynGAP

Primers were designed as described (Apperson et al., 1996). First strand cDNAs prepared from 5-week-old rat forebrain polyA+ RNA were amplified with the RT-for-PCR kit (Clontech, Palo Alto, CA) according to the manufacturer's protocol. Primers that resulted in successful amplification (Figure 2) were 5′-ACI CA(A/G) TA(T/C) GTI CA(T/C) TCI CCI TA(T/C) GA(T/C) CGI CC-3′ encoding a portion of peptide 9, and 5′-TC GGA TCC IC(G/T) IGC (T/C)TC IAT IAT CC-3′ antisense for a portion of peptide 14. PCR products were subcloned into the pCR2.1 plasmid supplied with the TA Cloning kit (Invitrogen, San Diego, CA). The ends of PCR products were sequenced to determine which encoded the entire sequences of the peptides that were partially encoded by the primers.

A λgt11 rat brain 5′-Stretch Plus cDNA library (Clontech) was screened for clones hybridizing with the initial PCR product (Figure 2B). A second screen was performed with a 280 bp probe that was amplified by PCR from the 3′ end of a cDNA obtained in the first screen. A total of 12 independent overlapping positive clones were plaque purified and cDNA inserts were subcloned into pBluescript (Stratagene, La Jolla, CA) for sequencing on an automated DNA sequencer in the Caltech DNA Microsequencing Facility. Overlapping sequences were assembled with Lasergene software (DNAStar, Madison, WI). Both strands of each cDNA were sequenced. All sequences contained within the open reading frame were present in more than one cDNA with the exception of the two putative alternatively spliced 5′ ends encoding the amino terminus. These alternative 5′ sequences were each found in single cDNAs that extended several hundred base pairs into the common open reading frame. The predicted splice junctions for the carboxy-terminal variants contained alternative splicing consensus sequences and did not contain EcoRI sites.

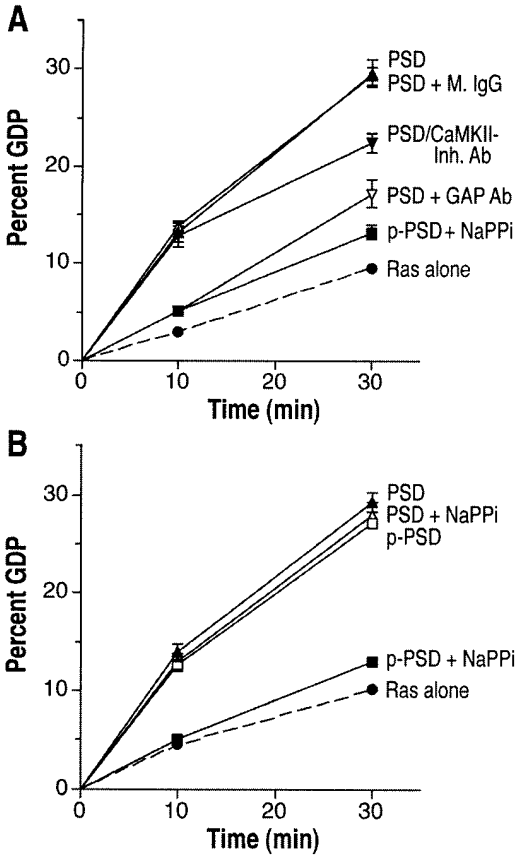

Figure 8. Inhibition of p135 SynGAP by CaMKII

(A) Inhibition of GAP activity in isolated PSDs after phosphorylation by CaMKII. RasGAP assays were performed for 10 or 30 min in the presence of Ras alone (closed circles), PSDs (30 μg; closed triangles), PSDs (30 μg) + 20 μg nonimmune mouse IgG (open upright triangles), PSDs (30 μg) + 20 μl anti-GAP ascites (open inverted triangles), PSDs (30 μg) prephosphorylated for 2 min in the presence of Ca^{2+}/CaM (closed squares), and PSDs prephosphorylated for 2 min in the presence of Ca^{2+}/CaM and inhibiting antibodies against CaMKII (as in Figure 7A; closed inverted triangles). After prephosphorylation of PSDs, CaM kinase activity and phosphatase activity were stopped by addition of 2 mM EGTA and 10 mM $NaPP_i$ immediately before addition of PSDs to the RasGAP assay. Note that the slight inhibition of GAP activity evident at 30 min in the GAP assay after prephosphorylation with inhibiting antibodies might result from slow phosphorylation during the GAP assay because the inhibiting antibodies do not completely block formation of autophosphorylated, Ca^{2+}-independent CaMKII during the prephosphorylation (Figure 7A; data not shown).

(B) Reversal of inhibition of RasGAP activity in the absence of phosphatase inhibitor. GTPase assays were performed as in (A) in the absence or presence of $NaPP_i$. Data are shown for Ras alone (closed circles), PSDs − $NaPP_i$ (closed upright triangles), PSDs + $NaPP_i$ (open upright triangles), prephosphorylated PSDs − $NaPP_i$ (open squres), prephosphorylated PSDs + $NaPP_i$ (closed squares). Data are plotted as mean ± SEM. In some instances, the error bars are not visible because they are smaller than the symbol.

Construction of Fusion Proteins and Preparation of Specific Antisera

Vectors encoding fusion proteins between glutathione S-transferase and the GAP domain (GST-GAP), and between GST and residues 17–85 of p135 SynGAP (GST-Nsp1), were constructed in pGEX-5X-1 (Pharmacia Biotech, Piscataway, NJ). Fusion proteins were expressed in *E. coli* and purified (Smith and Corcoran, 1995). Mice were immunized with each fusion protein to produce ascites fluids containing polyclonal antibodies (Ou et al., 1993). Immunoblots were prepared as described (Cho et al., 1992) and probed for 1 hr with mouse ascites fluid diluted to 1:2500.

Immunoprecipitation of p135 SynGAP

PSD protein (100 μg) was solubilized and immunoprecipitated (Lau et al., 1996) with antibodies specific for p135 SynGAP (anti-GAP domain and anti-NSP1 described above). Immunoblots of the precipitated proteins were prepared with the same antibodies, with rabbit serum against NR2B (Kornau et al., 1995) or with affinity-purified rabbit serum against PSD-95 (Cho et al., 1992).

Yeast Two-Hybrid Assays

Fragments of p135 SynGAP cDNA encoding amino acids 761 to 1293 of the principal splice variant (+QTRV) and amino acids 761 to 1270 of the carboxy-terminal splice variant shown in Figure 3Ab (−QTRV; Figure 5C) were inserted into the pAS2–1 yeast bait vector. Yeast two-hybrid assays were carried out according to the manufacturer's instructions (Clontech) with the prey vector pACT2 encoding a fusion with full-length PSD-95 (Cho et al., 1992). Interaction was measured by the β-galactosidase assay in intact yeast colonies. Hybrids containing +QTRV bait vector turned blue within 1 hr as did positive controls (Clontech). Hybrids containing −QTRV bait vector did not turn blue even after several hours.

Dissociated Hippocampal Cultures

Cultures of embryonic day 18 rat hippocampal neurons were grown as described (Brewer et al., 1993). After 2–4 weeks, cultures were fixed and labeled (Kornau et al., 1995; Apperson et al., 1996) with anti-GST-GAP at 1:500 and anti-NR2B rabbit antiserum at 1:1,000 (Kornau et al., 1995). Cultures were viewed in a Zeiss LSM310 fluorescence laser-scanning confocal microscope with a 63× oil immersion objective (Kornau et al., 1995).

Assays for Phosphorylation by CaMKII

Isolated PSDs prepared as described above were phosphorylated as previously described (Miller and Kennedy, 1985) in either 0 mM $CaCl_2$ or in 0.3 mM free Ca^{2+} and 0.1 mM [γ-^{32}P]ATP (2,500–10,000 cpm/pmol) for 2 min at 30°C. Phosphoproteins were fractionated by SDS-PAGE and visualized by autoradiography. In some reactions, inhibiting antibodies 4A11 and 6E9 (Molloy and Kennedy, 1991) against CaMKII (20 μg each of ascites IgG partially purified by precipitation with 50% ammonium sulfate) were included.

For immunoprecipitation, the reaction was adjusted to 50 mM Tris-HCl (pH 8.0), 150 mM NaCl, 1% NP-40, 0.5% sodium deoxycholate, and 0.8% SDS and was precleared by incubation with 100 μg protein A-agarose beads (Pierce, Rockford, IL) at 4°C for 1 hr. Precleared supernatant (10 μg) was incubated at 0.25 μg/μl with 5–15 μl anti-GST-GAP ascites at 4°C for 1 hr at a final concentration of 0.25% SDS. Aggregates were removed by centrifugation, and supernatant was incubated with 60 μg prewashed protein A-agarose beads at 4°C for 2 hr. Beads were pelleted and the supernatant was saved. Beads were washed five times with 50 mM Tris-HCl (pH 8.0), 150 mM NaCl, 1% NP-40, 0.5% sodium deoxycholate, and 0.1% SDS. Equivalent amounts of precleared starting material, supernatant, and beads were boiled 5 min in SDS sample buffer and applied to a 7.5% SDS-PAGE minigel. The gel was stained with Coomassie R-250, dried, and subjected to autoradiography. To estimate the percentage of radioactivity in the 135–150 kDa region of the gel that was immunoprecipitated with anti-GAP antibody, the appropriate gel bands were located by autoradiography, and cut from the dried gel, and their radioactivity was measured as Cerenkov radiation in a scintillation counter.

Assays for Ras-GTPase Activating Activity

Rat *c-H-Ras1* cDNA, with engineered EcoRI and XhoI restriction sites at 5′ and 3′ ends, respectively, was amplified by RT-PCR and inserted into pGEX-5X-1. The sequence of *c-H-Ras1* cDNA was confirmed by automated DNA sequencing. GST-Ras was expressed in *E. coli*, purified (Smith and Corcoran, 1995), dialyzed against 30 μM GDP, and stored at −20°C (Campbell-Burk and Carpenter, 1995). Ras bound to [γ-^{32}P]GTP (3,000 Ci/mM, ICN Pharmaceuticals, Irvine,

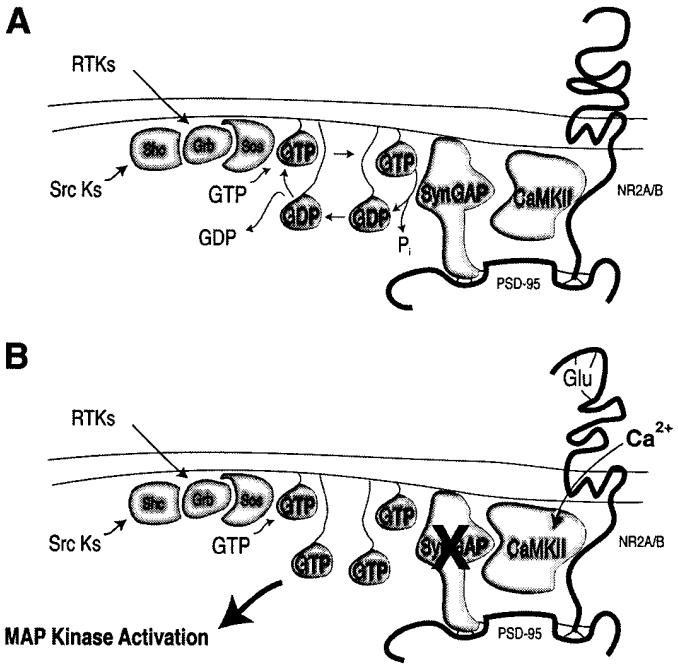

Figure 9. Cartoon of Hypothesized Effects of Regulation of p135 SynGAP by NMDA-Receptor Activation at Glutamatergic Synapses

(A) A variety of hormonal influences, including those that work via receptor tyrosine kinases (RTKs) and Src family kinases (Src Ks) feed into the Ras pathway by activating exchange of GTP for GDP bound to Ras. Active p135 SynGAP at postsynaptic densities will keep the steady-state level of active Ras low near the synapse by catalyzing rapid hydrolysis of Ras-GTP to Ras-GDP.

(B) Activation of NMDA receptors produces an influx of Ca^{2+} that activates CaMKII at the postsynaptic density. CaMKII then phosphorylates and inactivates p135 SynGAP, releasing the brake on the accumulation of active Ras-GTP and leading to increased activation of the MAP kinase cascade. In this manner, activation of the NMDA receptor may potentiate the action of any signal that leads to formation of Ras-GTP. Such potentiation would constitute yet another form of coincidence detection by the NMDA-type glutamate receptor.

CA) was prepared as described (Gibbs et al., 1988) except that binding was performed at 25°C for 15 min.

To measure the effect of phosphorylation on GAP activity, PSDs (one triton fraction prepared as described above) were prephosphorylated for 2 min as described above, and the assays were stopped by addition of 2 mM EGTA (to chelate free Ca^{2+}) with or without 20 mM $NaPP_i$ (to inhibit phosphatase activity) as indicated in the figure legends.

GTPase assays were initiated by addition of 2 pmol GTP-bound Ras (in 6 μl) to 60 μl of a mixture (Bollag and McCormick, 1995) containing 20–30 μg PSD protein, 45 mM Tris-HCl, 10 mM $MgCl_2$, 3 mM dithiothreitol, 100 mM NaCl, 0.1% NP-40, 1.2 mM EGTA, plus or minus 0.35 mM $CaCl_2$ (free $Ca^{2+} < 10^{-7}$ M), plus or minus 4 μM calmodulin, and plus or minus 9–10 mM Na pyrophosphate, the latter three depending upon prior phosphorylation conditions. The reactions were incubated at 25°C, stopped by addition of 300 μl ice-cold 10% glutathione-agarose beads (Sigma, St. Louis, MO), and incubated with stirring at 4°C for 45 min. Beads were washed (Smith and Corcoran, 1995) three times and nucleotides were dissociated from Ras on the beads for determination of percent GDP (GDP/[GDP + GTP] × 100) by thin layer chromatography (Bollag and McCormick, 1995). For inhibition of GAP activity by anti-GAP antibody, PSD proteins (20–30 μg) and mouse anti-GAP antibody (20 μl) or nonimmune mouse IgG (20 μg) were preincubated for 1 hr at 0°C and then warmed to 25°C for assay.

Acknowledgments

We thank L. Schenker for technical assistance and Gary Hathaway and Dirk Krapf of the Caltech microsequencing facility for mass spectrometric measurements and amino acid sequences. This work was supported by U.S. Public Health Service grants NS-28710 and 17660. A preliminary report of these findings was published in abstract form: Chen, H.-J., and Kennedy, M. B. (1997, Soc. Neurosci., abstract).

Received March 26, 1998; revised April 13, 1998.

References

Apperson, M.L., Moon, I.-S., and Kennedy, M.B. (1996). Characterization of densin-180, a new brain-specific synaptic protein of the O-sialoglycoprotein family. J. Neurosci. *16*, 6839–6852.

Bading, H., and Greenberg, M.E. (1991). Stimulation of protein tyrosine phosphorylation by NMDA receptor activation. Science *253*, 912–914.

Bading, H., Ginty, D.D., and Greenberg, M.E. (1993). Regulation of gene expression in hippocampal neurons by distinct calcium signaling pathways. Science *260*, 181–186.

Bollag, G., and McCormick, F. (1995). Intrinsic and GTPase-activating protein-stimulated Ras GTPase assays. Methods Enzymol. *255*, 161–170.

Brewer, G.J., Torricelli, J.R., Evege, E.K., and Price, P.J. (1993). Optimized survival of hippocampal neurons in B27-supplemented Neurobasal™, a new serum-free medium combination. J. Neurosci. Res. *35*, 567–576.

Cabelli, R.J., Shelton, D.L., Segal, R.A., and Shatz, C.J. (1997). Blockade of endogenous ligands of trkB inhibits formation of ocular dominance columns. Neuron *19*, 63–76.

Campbell-Burk, S.L., and Carpenter, J.W. (1995). Refolding and purification of Ras proteins. Methods Enzymol. *255*, 3–13.

Carlin, R.K., Grab, D.J., Cohen, R.S., and Siekevitz, P. (1980). Isolation and characterization of postsynaptic densities from various brain regions: enrichment of different types of postsynaptic densities. J. Cell Biol. *86*, 831–843.

Cho, K.-O., Hunt, C.A., and Kennedy, M.B. (1992). The rat brain postsynaptic density fraction contains a homolog of the Drosophila discs-large tumor suppressor protein. Neuron *9*, 929–942.

Cobb, M.H., and Goldsmith, E.J. (1995). How MAP kinases are regulated. J. Biol. Chem. *270*, 14843–14846.

Cohen, G.B., Ren, R.B., and Baltimore, D. (1995). Modular binding domains in signal-transduction proteins. Cell *80*, 237–248.

Downward, J., Graves, J.D., Warne, P.H., Rayter, S., and Cantrell, D.A. (1990). Stimulation of p21ras upon T-cell activation. Nature *346*, 719–723.

English, J.D., and Sweatt, J.D. (1996). Activation of p42 mitogen-activated protein kinase in hippocampal long term potentiation. J. Biol. Chem. *271*, 24329–24332.

English, J.D., and Sweatt, J.D. (1997). A requirement for the mitogen-activated protein kinase cascade in hippocampal long term potentiation. J. Biol. Chem. *272*, 19103–19106.

Erondu, N.E., and Kennedy, M.B. (1985). Regional distribution of type II Ca^{2+}/calmodulin-dependent protein kinase in rat brain. J. Neurosci. *5*, 3270–3277.

Farnsworth, C.L., Freshney, N.W., Rosen, L.B., Ghosh, A., Greenberg, M.E., and Feig, L.A. (1995). Calcium activation of Ras mediated by neuronal exchange factor Ras-GRF. Nature *376*, 524–527.

Finkbeiner, S., and Greenberg, M.E. (1996). Ca^{2+}-dependent routes to Ras: mechanisms for neuronal survival, differentiation, and plasticity? Neuron *16*, 233–236.

Fukunaga, K., Soderling, T.R., and Miyamoto, E. (1992). Activation of Ca^{2+}/calmodulin-dependent protein kinase II and protein kinase C by glutamate in cultured rat hippocampal neurons. J. Biol. Chem. *267*, 22527–22533.

Fukunaga, K., Stoppini, L., Miyamoto, E., and Muller, D. (1993). Long-term potentiation is associated with an increased activity of Ca^{2+}/calmodulin-dependent protein kinase II. J. Biol. Chem. *268*, 7863–7867.

Ghosh, A., and Greenberg, M.E. (1995). Calcium signaling in neurons: molecular mechanisms and cellular consequences. Science *268*, 239–247.

Gibbs, J.B., Schaber, M.D., Allard, W.J., Sigal, I.S., and Scolnick, E.M. (1988). Purification of ras GTPase activating protein from bovine brain. Proc. Natl. Acad. Sci. USA *85*, 5026–5030.

Grant, S.G., O'Dell, T.J., Karl, K.A., Stein, P.L., Soriano, P., and Kandel, E.R. (1992). Impaired long-term potentiation, spatial learning, and hippocampal development in fyn mutant mice. Science *258*, 1903–1910.

Hellman, U., Wernstedt, C., Gonez, J., and Heldin, C.-H. (1995). Improvement of an "in-gel" digestion procedure for the micropreparation of internal protein fragments for amino acid sequencing. Anal. Biochem. *224*, 451–455.

Hsueh, Y.-P., Kim, E., and Sheng, M. (1997). Disulfide-linked head-to-head multimerization in the mechanism of ion channel clustering by PSD-95. Neuron *18*, 803–814.

Irie, M., Hata, Y., Takeuchi, M., Ichtchenko, A., Toyoda, A., Hirao, K., Takai, Y., Rosahl, T.W., and Sudhof, T.C. (1997). Binding of neuroligins to PSD-95. Science *277*, 1511–1515.

Kang, H., and Schuman, E.M. (1995). Long-lasting neurotrophin-induced enhancement of synaptic transmission in the adult hippocampus. Science *267*, 1658–1662.

Kelly, P.T., McGuinness, T.L., and Greengard, P. (1984). Evidence that the major postsynaptic density protein is a component of a Ca^{2+}/calmodulin-dependent protein kinase. Proc. Natl. Acad. Sci. USA *81*, 945–949.

Kennedy, M.B. (1997). The postsynaptic density at glutamatergic synapses. Trends Neurosci. *20*, 264–268.

Kennedy, M.B., Bennett, M.K., and Erondu, N.E. (1983). Biochemical and immunochemical evidence that the "major postsynaptic density protein" is a subunit of a calmodulin-dependent protein kinase. Proc. Natl. Acad. Sci. USA *80*, 7357–7361.

Kim, J.H., Liao, D., Lau, L-F., and Huganir, R.L. (1998). SynGAP: a synaptic RasGAP that associates with the PSD-95/SAP90 protein family. Neuron *20*, 683–691.

Kornau, H.-C., Schenker, L.T., Kennedy, M.B., and Seeburg, P.H. (1995). Domain interaction between NMDA receptor subunits and the postsynaptic density protein PSD-95. Science *269*, 1737–1740.

Lau, L.F., Mammen, A., Ehlers, M.D., Kindler, S., Chung, W.J., Garner, C.C., and Huganir, R.L. (1996). Interaction of the N-methyl-D-aspartate receptor complex with a novel synapse-associated protein, sap102. J. Biol. Chem. *271*, 21622–21628.

Lemmon, M.A., Falasca, M., Ferguson, K.M., and Schlessinger, J. (1997). Regulatory recruitment of signaling molecules to the cell-membrane by pleckstrin-homology domains. Trends Cell Biol. *7*, 237–242.

Lu, Y.M., Roder, J.C., Davidow, J., and Salter, M.W. (1998). Src activation in the induction of long-term potentiation in CA1 hippocampal neurons. Science *279*, 1363–1367.

Mayford, M., Wang, J., Kandel, E.R., and O'Dell, T.J. (1995). CaMKII regulates the frequency-response function of hippocampal synapses for the production of both LTD and LTP. Cell *81*, 891–904.

McAllister, A.K., Katz, L.C., and Lo, D.C. (1997). Opposing roles for endogenous BDNF and NT-3 in regulating cortical dendritic growth. Neuron *18*, 767–778.

Miller, S.G., and Kennedy, M.B. (1985). Distinct forebrain and cerebellar isozymes of type II Ca^{2+}/calmodulin-dependent protein kinase associate differently with the postsynaptic density fraction. J. Biol. Chem. *260*, 9039–9046.

Molloy, S.S., and Kennedy, M.B. (1991). Autophosphorylation of type II Ca^{2+}/calmodulin-dependent protein kinase in cultures of postnatal rat hippocampal slices. Proc. Natl. Acad. Sci. USA *88*, 4756–4760.

Moon, I.S., Apperson, M.L., and Kennedy, M.B. (1994). The major tyrosine-phosphorylated protein in the postsynaptic density fraction is *N*-methyl-D-aspartate receptor subunit 2B. Proc. Natl. Acad. Sci. USA *91*, 3954–3958.

Nakamura, T., Muraoka, S., Sanokawa, R., and Mori, N. (1998). N-Shc and Sck, Two neuronally expressed Shc adapter homologs. Their differential regional expression in the brain and roles in neurotrophin and src signaling. J. Biol. Chem. *273*, 6960–6967.

Niethammer, M., Kim, E., and Sheng, M. (1996). Interaction between the C-terminus of NMDA receptor subunits and multiple members of the PSD-95 family of membrane-associated guanylate kinases. J. Neurosci. *16*, 2157–2163.

Omkumar, R.V., Kiely, M.J., Rosenstein, A.J., Min, K.-T., and Kennedy, M.B. (1996). Identification of a phosphorylation site for calcium/calmodulin-dependent protein kinase II in the NR2B subunit of the N-methyl-D-aspartate receptor. J. Biol. Chem. *271*, 31670–31678.

Ou, S.K., Hwang, J.M., and Patterson, P.H. (1993). A modified method for obtaining large amounts of high-titer polyclonal Ascites fluid. J. Immunol. Methods *165*, 75–80.

Ouyang, Y., Kantor, D., Harris, K.M., Schuman, E.M., and Kennedy, M.B. (1997). Visualization of the distribution of autophosphorylated calcium/calmodulin-dependent protein kinase II after tetanic stimulation in the CA1 area of the hippocampus. J. Neurosci. *17*, 5416–5427.

Prakash, N., Cohen-Cory, S., and Frostig, R.D. (1996). Rapid and opposite effects of BDNF and NGF on the functional organization of the adult cortex in vivo. Nature *381*, 702–706.

Rao, A., and Craig, A.M. (1997). Activity regulates the synaptic localization of the NMDA receptor in hippocampal neurons. Neuron *19*, 801–812.

Rozakis-Adcock, M., McGlade, J., Mbamalu, G., Pelicci, G., Day, R., Li, W., Batzer, A., Thomas, S., Brugge, J., Pelicci, P.G., et al. (1992). Association of the Shc and Grb2/Sem5 SH2-containing proteins is implicated in activation of the Ras pathway by tyrosine kinases. Nature *360*, 689–692.

Scheffzek, K., Lautwein, A., Kabsch, W., Ahmadian, M.R., and Wittinghofer, A. (1996). Crystal structure of the GTPase-activating domain of human p120GAP and implications for the interaction with Ras. Nature *384*, 591–596.

Schuman, E.M. (1997). Synapse specificity and long-term information storage. Neuron *18*, 339–342.

Sheng, M. (1996). PDZs and receptor/channel clustering: rounding up the latest suspects. Neuron *17*, 575–578.

Shields, S.M., Ingebritsen, T.S., and Kelly, P.T. (1985). Identification of protein phosphatase-1 in synaptic junctions—dephosphorylaton of endogenous calmodulin-dependent kinase II and synapse-enriched phosphoproteins. J. Neurosci. *5*, 3414–3422.

Silva, A.J., Stevens, C.F., Tonegawa, S., and Wang, Y. (1992). Deficient hippocampal long-term potentiation in α-calcium-calmodulin kinase II mutant mice. Science *257*, 201–206.

Smith, D.B., and Corcoran, L.M. (1995). Protein Expression. In Current Protocols in Molecular Biology, F.M. Ausubel, R. Brent, R.E. Kingston, D.D. Moore, J.G. Seidman, J.A. Smith, and K. Struhl, eds. New York: Wiley Interscience), pp. 1671–1677.

Südhof, T.C., and Rizo, J. (1996). Synaptotagmins: C2-domain proteins that regulate membrane traffic. Neuron *17*, 379–388.

Trahey, M., Wong, G., Halenbeck, R., Rubinfeld, B., Martin, G.A., Ladner, M., Long, C.M., Crosier, W.J., Watt, K., Koths, K., et al. (1988). Molecular cloning of two types of GAP complementary DNA from human placenta. Science *242*, 1697–1700.

Vogel, U.S., Dixon, R.A.F., Schaber, M.D., Diehl, R.E., Marshall, M.S., Scolnick, E.M., Sigal, I.S., and Gibbs, J.B. (1988). Cloning of bovine GAP and its interaction with oncogenic ras-p21. Nature *335*, 90–93.

Wigler, M.H. (1990). GAPs in understanding Ras. Nature *346*, 696–697.

Xia, X., Dudek, H., Miranti, C.K., and Greenberg, M.E. (1996). Calcium influx via the NMDA receptor induces immediate early gene transcription by a MAP kinase/ERK-dependent mechanism. J. Neurosci. *16*, 5425–5436.